Propagation of Rarefaction Pulses in Discrete Materials with Strain-Softening Behavior

E. B. Herbold and V. F. Nesterenko

Propagation of Rarefaction Pulses in Discrete Materials with Strain-Softening Behavior

E.B. Herbold[1], V.F. Nesterenko[2, 3]

[1]*Lawrence Livermore National Laboratory, L-286, P.O. Box 808, Livermore, CA 94550, USA.*

[2]*Department of Mechanical and Aerospace Engineering,*

University of California at San Diego, La Jolla, California 92093-0411, USA

[3]*Materials Science and Engineering Program,*

University of California at San Diego, La Jolla, California 92093-0418, USA

(Date: January 22, 2013)

We report on the dynamic behavior of strongly nonlinear discrete materials with anomalous strain softening behavior. Rarefaction solitary waves found in numerical calculations agree well with the exact solution to the continuum wave equation. Compression pulses generated by impact quickly disintegrate into a leading rarefaction solitary wave followed by an oscillatory wave train containing localized excitations. Such behavior is favorable for metamaterials design of shock absorption layers as well as tunable information transmission lines for scrambling of acoustic information.

Discrete periodic materials with a "normal" power-law relationship between force and displacement, $F \propto \delta^n$ for $n > 1$, have been shown to support compression solitary waves [1-9]. When dynamic forces between masses are significantly larger than the initial force applied to the system, these materials exhibit strongly nonlinear behavior, which has been considered in recent investigations of shock mitigation barriers, waveguides for acoustic switches and rectification [3,4,6,10]. These materials can support compression solitary wave solutions traveling in one-dimensional chains or ordered two and three–dimensional arrays of particles [1,2]. Conversely, a discrete chain with an interaction law exhibiting a general softening behavior (first considered in [11]) supports rarefaction solitary waves and rarefaction shock-like waves if dissipation is present [2]. Stationary rarefaction waves were investigated in magnetized Hall plasmas and are thought to explain observed anomalous behavior due to a changing electric field [12]. Depression solitary waves have also been investigated previously in liquid Hg [13].

An elastic or viscoelastic softening behavior is exhibited by a decreasing of elastic modulus with strain in a wide range of materials ranging from polymer foams [14,15] and rubber [16,17] to actin networks in biological tissues [18,19]. In general, these materials share several common characteristics under compressive loading: a viscoelastic softening behavior due to configuration changes in polymer chains [15,16,17,20] or the elastic collapse of cell-wall structures in polymer foams [14, 21-24]. Both softening phenomena are followed by a stiffening behavior attributed to the bulk resistance to further deformation.

Here, we consider a simple one-dimensional metamaterial composed of point masses interacting with a force-displacement relationship, $F \propto \delta^n$ for $n < 1$. For example, these

materials can be assembled in a chain from stainless steel cylinders separated by flat layers of low-density polymer foam or solid rubber. In this case, the "rigid" steel cylinders can be considered as point masses m connected by a "soft" and massless nonlinear spring. Analogous strongly nonlinear metamaterials have recently been investigated with stainless steel cylinders separated by polymer o-rings [7,8,25,26]. The Hamiltonian of this system may be written in terms of the displacement of the cylinders, u_i, $H = \sum_i \left[\frac{m\dot{u}_i^2}{2} + U(\delta_{i,i+1}) \right]$ where $\delta_{i,i+1} = u_i - u_{i+1}$. The potential energy of interacting i-th and $(i+1)$-th particles is defined as

$$U(\delta_{i,i+1}) = K_{i,i+1}/(n+1) \left\{ (\delta_{i,i+1} + s_{i,i+1})^{n+1} - s_{i,i+1}^n \left[(n+1)\delta_{i,i+1} + s_{i,i+1} \right] \right\}_+ \quad (1)$$

where the '+' outside of the curly brackets indicate that only positive values of relative displacement, δ, are taken and $K_{i,i+1}$ is the effective stiffness constant corresponding to the power law interaction between the i-th and $(i+1)$-th particles. The parameter 's' in Eq. (1) is introduced to account for initial slope of the force displacement relationship for the 'i'th location ($F = -dU(\delta)/d\delta$). The resulting equation of motion is,

$$\ddot{u}_i = A_{i-1,i} \left[(\delta_{i-1,i} + s_{i-1,i})^n - s_{i-1,i}^n \right]_+ - A_{i,i+1} \left[(\delta_{i,i+1} + s_{i,i+1})^n - s_{i,i+1}^n \right]_+ \quad (2)$$

where $A_{i-1,i} = K_{i-1,i}/m$ and $0 < n < 1$. Initial displacements caused by an external force may also be included in u_i. This form of the force-displacement relationship, when cast as stress and strain, is very similar to the simple power law model for the compression of solid rubber found in [15,16].

The long–wave approximation for Eq. (2) is derived assuming that the distance between centers of masses, a, is significantly less than the characteristic length of propagating wave L. To simplify the following discussion it will be assumed that

parameters m, A and s are uniform. The long wave approximation to Eq. (2) is presented below,

$$u_{tt} = -c_n^2 \left\{ \left(\frac{s}{a} - u_x\right)^n + \frac{na^2}{6(n+1)} \left[\left(\frac{s}{a} - u_x\right)^{(n-1)/2} \left(\left(\frac{s}{a} - u_x\right)^{(n+1)/2}\right)_{xx} \right] \right\}_x, \qquad (3)$$

where $c_n^2 = Aa^{n+1}$ is a parameter with units of speed. The long wave sound speed c_0 in the chain of particles is found through the linearization of Eq. (3), $c_0^2 = nc_n^2(\xi_0 + s/a)^{n-1}$. Equation (3) may be reduced to a nonlinear ordinary differential equation for the specific case of a stationary wave propagating with speed V,

$$y_{\eta\eta} + y - y^{-\frac{(n-3)}{(n+1)}} + y^{-\frac{(n-1)}{(n+1)}}C = 0, \qquad (4)$$

for arbitrary values of n. In Eq. (4), y is a reduced form of the strain ($\xi = -u_x$), $y = (c_n/V)^{(n+1)/(n-1)}(s/a + \xi)^{(n+1)/2}$, C is a constant and η is the normalized coordinate $\eta = x/a\sqrt{6(n+1)/n}$.

Eq. (4) can be rewritten as an equation for a nonlinear oscillator moving in an effective "potential field", $d^2y/d\eta^2 = -dW(y)/dy$ where $W(y)$ is defined as

$$W(y) = \frac{1}{2}y^2 - \frac{n+1}{4}y^{\frac{4}{(n+1)}} + C_1 y^{\frac{2}{(n+1)}}. \qquad (5)$$

For an anomalous interaction between particles, $0 < n < 1$, rarefaction solitary waves exist when $C_1 = C(n+1)/2$ is bound by [2, 11],

$$\frac{n^2-1}{2}n^{n/(1-n)} < C_1 \leq \frac{n-1}{2}\left(\frac{2n}{n+1}\right)^{\frac{n}{(1-n)}}. \qquad (6)$$

The value of C_1 defines system behavior between weakly and strongly nonlinear regimes corresponding to the lower and upper bound of C_1, respectively.

Three curves in Fig. 1(a) show the potential field $W(y)$ for the strongly (curve (1)) and weakly (curve (3)) nonlinear regimes. Along each of these curves we may consider that a

particle moves from its initial position in the wave (y_1, corresponding to ξ_0) to y_{min} (related to ξ_{min}) and back to y_1 (Fig.1 (a)). An interesting value of y_1 corresponds to the case where the minimum of y is equal to zero, which results in an expression that depends only on the power-law exponent, $y_1 = (2n/n+1)^{(1+n)/2(1-n)}$ [2,11]. This special case is shown in curve (1) with $n = 1/2$, $C_1 = -1/6$ (the upper bound of C_1 in Eq. (6)) and $y_1 = (2/3)^{3/2}$. The variations in y are relatively large in strongly nonlinear regimes (see curves (1) and (2) in Fig. 1 (a)) and may be infinitesimally small in the weakly nonlinear regime (see curve (3)) near the lower bound value of $C_1 = -0.1875$ (for $n=1/2$).

Figure 1 (b) shows the numerical solution of Eq. (4) for the three values of C (where $C = C_1 2/(n+1)$) corresponds to the curves in Fig. 1 (a). The width of the wave increases in the weakly nonlinear case compared to the strongly nonlinear case (compare curves 1 and 2 to curve 3 in Fig. 1 (b)). Also, the shape of a strongly nonlinear solitary wave with minimum strain equal to zero (when $s=0$) is similar to solitary waves with finite minimum strain (compare curves (1) and (2)).

It is interesting that a strain perturbation solution of Eq. (3), (i.e. $\xi=\xi_0+\Delta\xi$), results in a KdV type depression solitary wave similar to found in [13]. The weakly nonlinear solution is $\xi = \xi_0 - \Delta\xi\,\text{sech}^2((x - Vt)/L)$ for $n<1$ where $\Delta\xi = 6c_0(V + c_0)/\tau$, $L = \sqrt{12\alpha/(\tau\Delta\xi)}$, $\tau = (1 - n)c_0^2/(\xi_0 + s_0/a)$, $\alpha = a^2c_0^2/12$. This also means that these depression solitary waves are partial solutions to the system described here. It should be mentioned that the interaction law between neighboring particles in Eq. (2) is assumed non-dissipative. We are primarily investigating the solitary wave structure, which may be weakly attenuating with dissipation but still preserving its main features as in [13] or

be accompanied by a secondary shock-like wave structure as in [27], which would require a separate investigation.

The exact solution for the long wave approximation can be found for the case where the minimum value of y is equal to zero and C_1 is given by the maximum value in Eq. (6). In the system of reference moving with the wave and centered at the minimum value of strain, an exact solution can be obtained for $n = 1/2$ and $C_1 = -1/6$ by substituting Eq. (5) into $\eta = \int_0^y dy/\sqrt{-2W(y)}$ giving,

$$y = (2/3)^{3/2}\left|\tanh^3\left(\sqrt{2}\eta/6\right)\right|. \tag{7}$$

The corresponding equation for the strain is (for $s=0$),

$$\xi = \xi_0 \tanh^4(x/a). \tag{8}$$

The exact solution in Eqs. (7) and (8) predicts a symmetric cup-shaped pulse with a characteristic pulse length equal to $7a$ for a cut-off of $\xi/\xi_0 = 0.98$. The pulse width does not depend on the amplitude of the solitary wave similar to the case for compressive solitary waves in a "sonic vacuum" where $n>1$ [2]. Equation (7) is shown in Fig. 1(b), curve (1), for $n=1/2$. In contrast to the strongly nonlinear compression wave in a sonic vacuum, the strongly nonlinear rarefaction waves defined by Eqs. (7) and (8) are not "compact" solitary waves.

A closed form expression may be constructed for strongly nonlinear solitary rarefaction waves for values of $0<n<1$. Here, the amplitude is equal to the value of y_1 and the width of the wave depends on values of n,

$$y = \left(\frac{2n}{n+1}\right)^{(1+n)/2(1-n)}\left|\tanh^{(1+n)/n}\left(\frac{\eta}{\sqrt{3(n+1)/(n(1-n))}}\right)\right|. \tag{9}$$

The full width at half-maximum (FWHM) in terms of x/a is easily found for Eq. (9),

FWHM $= \sqrt{2/(1-n)}\,\text{arctanh}\left[2^{\frac{-n}{1+n}}\right]$. Interestingly, a minimum value of this FWHM

corresponds to $n=0.38$ where $x/a=2.113$. It is also interesting to find the relationships

between the phase speed V and the strain ξ. The phase speed can be found using the

properties of the potential function; $W(y=y_{min}) = W(y=y_1)$ and $\partial W/\partial y\big|_{y=y_1} = 0$, giving,

$$V_r = \frac{c_n}{\xi_0 - \xi_{min}}\left\{\frac{2\left[n(s/a+\xi_0)^{n+1}+(s/a+\xi_{min})^{n+1}-(n+1)(s/a+\xi_0)^n(s/a+\xi_{min})\right]}{n+1}\right\}^{1/2}. \quad (10)$$

In the case of a solitary rarefaction wave where $\xi_{min}=0$, Eq. (10) becomes,

$$V_{s,r} = \frac{c_n}{\xi_0}\left\{\frac{2\left[n\left(s/a+\xi_0\right)^{n+1}+\left(s/a\right)^{n+1}-s/a(n+1)\left(s/a+\xi_0\right)^n\right]}{n+1}\right\}^{1/2}. \quad (11)$$

The ratio of the solitary wave speed, $V_{s,r}$ to the sound speed c_0 is greater than 1 for

$0<n<1$, meaning the solitary rarefaction wave speed is supersonic [2].

The shape and speed of the wave in numerical calculations of a discrete chain must be

compared to Eqs. (8)-(11) since they were derived from the long-wave approximation.

The corresponding numerical calculations are performed in Matlab using ODE45 to

integrate the system of equations in Eq. (2). Energy is conserved within 10^{-10}% and

momentum is conserved within 10^{-12}% in each simulation. The boundary conditions are

such that the chain is initially compressed with an external constant force and the point

masses (with $m=5$g) are in their initial static positions due to the action of this force. The

force is held constant in time and the first particle is given an initial velocity to simulate

impulse loading directed either toward or against the rest of the chain. Each calculation

uses the constants for a uniform chain; $n=1/2$, $\xi_0=0.033$, $s=5\cdot10^{-5}$ m, and $A=1\cdot10^5$

N/m$^{1/2}$ unless specified otherwise. An experimentally reasonable value for a is 6mm

where the deformable element is 1mm and the rigid mass is 5mm in length. When the

deformable elements are strained by 20%, this gives ξ_0=0.033. Figure 2 shows the results

from simulations using 10001 discrete masses where constant force of F_0=4.37N is

applied to both the first and last particle. The first and last particles were given an initial

velocity v_0=-0.775 and 0.775m/s, which produces two colliding solitary rarefaction waves

with a minimum strain equal to zero (Fig. 2(a) corresponds to t=2.5s). The result of the

applied static compression force and specific initial velocities is the formation of two

solitary rarefaction waves. The rarefaction waves propagate faster than their oscillatory

wave trains and separate from it within approximately 80 particles. The minimum of the

left wave occurs at the 4927th and 4946st particles at 2.51s and 2.52s, respectively, giving

an average speed of 11.78 m/s, which differs from the predicted speed of 11.72 m/s from

Eq. (10) within 1%. Figure 2(b) demonstrates the inelastic scatter behind the two leading

pulses after the collision of two rarefaction solitary waves.   Figure 2(c) shows a

comparison between the right moving wave from Figs. 2(b) and a solitary rarefaction

wave traveling in a chain without a left-moving wave. The phase shift and oscillations

behind the main pulse are not present in the latter case.

It is important to validate the analytical expressions given in Eq. (7)-(9) by

comparison with the discrete simulations because the width of the solitary wave is

comparable to the distance between particles. Figure 3 shows this comparison for n=1/5,

1/2 and 4/5.   The same initial strain, stiffness value (A=$1 \cdot 10^5$ N/m^n), and slope

parameter (s=0) were used in each calculation. The force and velocity necessary for the

creation of a strongly nonlinear rarefaction wave were f_0=91 N, v_0=-1.69 m/s for n=1/5,

f_0=7.1 N, v_0=-0.729 m/s for n=1/2 and f_0=0.549 N, v_0=-0.313 m/s for n=4/5.   The

calculations for a discrete system show that there are approximately 7 particles

comprising the pulse for $n=1/2$ and $n=1/5$ and 9 particles for $n=4/5$. It is interesting that the difference between the discrete strain values and Eq. (9) is smaller for $n=4/5$ than for $n=1/2$, indicating that: (1) discreteness plays an important role which is clearly observed by comparison between the exact solution and numerical calculations for $n=1/2$ and (2) alternative approaches may be pursued to better approximate the pulse shape and wave speed to account for these differences [28].

An illustrative example of impact is shown in Fig. 4 where an impact velocity of 3 m/s was given to the first particle, to which a constant force is applied and the position of the last particle was fixed. The initial compression pulse quickly attenuates due to nonlinear dispersion and the first rarefaction pulse immediately behind it eventually becomes the leading pulse after traveling approximately 475 particles. This behavior is quite counterintuitive since impact loading is expected to result in compression pulse for "normal" materials.

The arrow (1) in Fig. 4 is pointing to a slowly moving wave packet (i.e. an envelope solitary wave) indicating that breather modes may exist in chains with an exponent $n<1$. This observation suggests that the presence of breather modes is not restricted to discrete chains with hardening power laws, where a periodic assembly or mass impurity is requisite [29-31]. Multiple types of waves may be supported by this system including KdV, envelope type and strongly nonlinear solitary and shock-like rarefaction waves which may be important for energy transport or new types of information carriers in electrical system analogs.

It is interesting that solitary rarefaction waves may arise by specifying a velocity toward or away from the rest of the chain and suggests different methods to test materials

experimentally. This is not possible for strongly nonlinear compression waves in granular media where $n>1$ due to the absence of a restoring force.

We investigated rarefaction waves in nonlinear periodic systems with a 'softening' general power-law relationship between force and displacement to understand the dynamic behavior of this class of metamaterials. An exact closed form expression describing the shape of the strongly nonlinear rarefaction wave for $n=1/2$ agrees well with numerical simulations of discrete system. The width of the investigated strongly nonlinear solitary wave does not depend on the amplitude and it is smallest for $n=0.38$ in investigated interval of values of n. The agreement between the theoretical and numerical pulse speed of the waves is within 1%. It was shown that the solitary wave speed was supersonic and is inversely proportional to the initial strain of the system. Impact on a compressed chain of particles generated a rarefaction solitary wave as the leading pulse.

REFERENCES

[1] V.F. Nesterenko, Prikl. Mekh. Tekh. Fiz. **5**, 136 (1983) [J. Appl. Mech. Tech. Phys., **5**, 733 (1984)].

[2] V. F. Nesterenko, Dynamics of Heterogeneous Materials (Springer-Verlag, New York, 2001).

[3] V. Nesterenko, Fizika Goreniya i Vzryva **28**, 121 (1992).

[4] G. Friesecke and J.A.D. Wattis, Commun. Math. Phys. **161**, 391 (1994).

[5] C. Coste, E. Falcon, and S. Fauve, Physical Review E **56**, 6104 (1997).

[6] C. Daraio, V.F. Nesterenko, E.B. Herbold, and S. Jin, Phys. Rev. E **72**, 016603 (2005).

[7] E.B. Herbold and V.F. Nesterenko, Appl. Phys. Lett. **90**, 261902 (2007).

[8] E.B. Herbold and V.F. Nesterenko, APS-Shock Comp. Cond. Matt., in: AIP Conf. Proc., Hawaii, HI, 231 (2007).

[9] Sen S., Hong J., Bang J., Avalos E., and Doney R., Phys. Rep., **462**, 21 (2008).

[10] N. Boechler, G. Theocharis, C. Daraio, Nature Mat., DOE:10.1038/NMAT3072 (2011).

[11] V.F. Nesterenko, Fizika Goreniya i Vzryva **29**, 134 (1993).

[12] A.S. Chuvatin, A.A. Ivanov, and L.I. Rudakov, Phys. Rev. Lett. **92**, 095007 (2004).

[13] E. Falcon, C. Laroche, S. Fauve, Phys. Rev. Lett. **89**, 204501 (2002).

[14] P.J. Blatz, and W.L. Ko, Trans. Soc. Rheol. **6**, 223 (1962).

[15] R.W. Ogden, Proc. R. Soc. Lond. A. **328**, 567 (1972).

[16] R.W. Ogden, Proc. R. Soc. Lond. A. **326**, 565 (1972).

[17] J.S. Bergstrom, M.C. Boyce, J. Mech. Phys. Solids, 46, 931 (1998).

[18] O. Chaudhuri, S.H. Parekh, and D.A. Fletcher, Nature **445**, 295 (2007).

[19] A. Kabla, and L. Mahadevan, J. R. Soc. Interface **4**, 99 (2007).

[20] L. Mullins, Rubber Chem. Technol. **42**, 339 (1969).

[21] D.M. Schwaber, and E.A. Meinecke, J. Appl. Polymer Sci. **15**, 2181 (1971).

[22] L.J. Gibson, M.F. Ashby, *Cellular solids: structure and properties* , Oxford, New York: Pergamon Press, (1988).

[23] J.W. Klintworth, and W.J. Stronge, Int. J. Mech. Sci. **30**, 273 (1988).

[24] F. Scarpa, L.G. Ciffo, and J.R. Yates, Smart Mater. Struct. **13**, 49 (2004).

[25] I. Lima Dias Pinto, A. Rosas, A.H. Romero, K. Lindenberg, Phys. Rev. E **82**, 031308 (2010).

[26] A. Spadoni, C. Daraio, W. Hurst, M. Brown, Appl. Phys. Lett, **98**, 161901 (2011).

[27] A. Rosas, A.H. Romero, V.F. Nesterenko, K. Lindenberg, Phys. Rev. Lett., **98**, 164301 (2007).

[28] A. Rosas, K. Lindenberg, Phys. Rev. E, **69**, 037601 (2004).

[29] T. Dauxois, M. Peyrard, Phys. Rev. Lett., **70**, 3935 (1993).

[30] G. Theocharis et. al, Phys. Rev. E **80**, 066601 (2009).

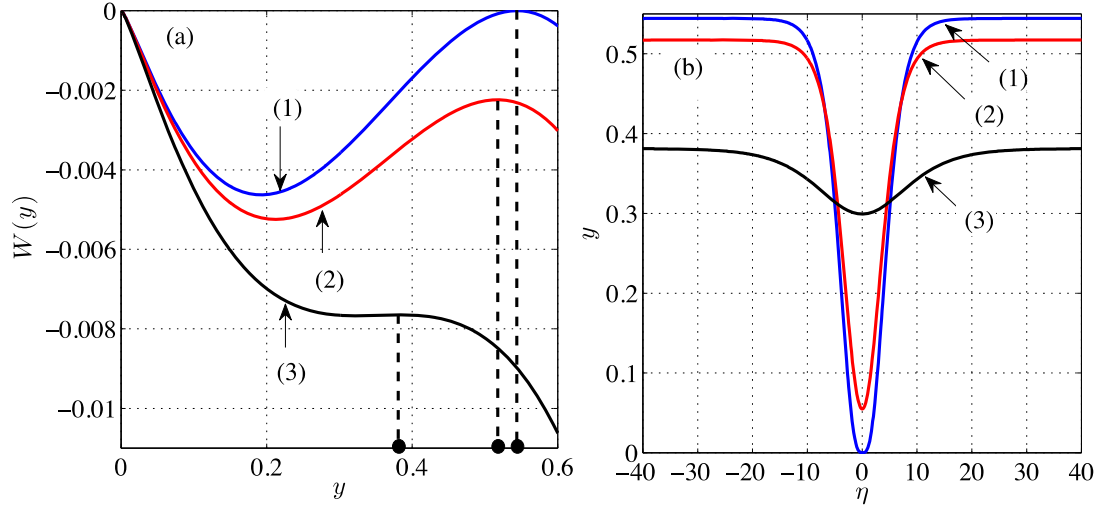[31] N. Boechler, G. Theocharis, S. Job, P. Kevrekidis, M. Porter, C. Daraio, Phys. Rev. Lett., **104**, 244302 (2010)

FIG. 1: (a) Three curves for different values of C_1 are shown for the potential function, Eq. (5), with $n = \frac{1}{2}$ Curve (1): $C_1 = -1/6$ and the value of y_1 corresponds to $(2/3)^{3/2}$. Curve (2): $C_1 = -11/64$ and $y_1 = 0.517$. Curve (3): $C_1 = -0.1869$ and $y_1 = 0.381$. (b) Solution of Eq. (4) for corresponding values of C. The width of the wave is larger for smaller values of C. Each curve starts at a different value of y_1 (shown by●in part (a)). Curve (1): $C = -2/9$, $y_1 = (2/3)^{3/2}$. Curve (2): $C = -11/48$, $y_1 = 0.517$. Curve (3): $C = -0.249$, $y_1 = 0.381$. All three curves have been shifted horizontally for comparison.
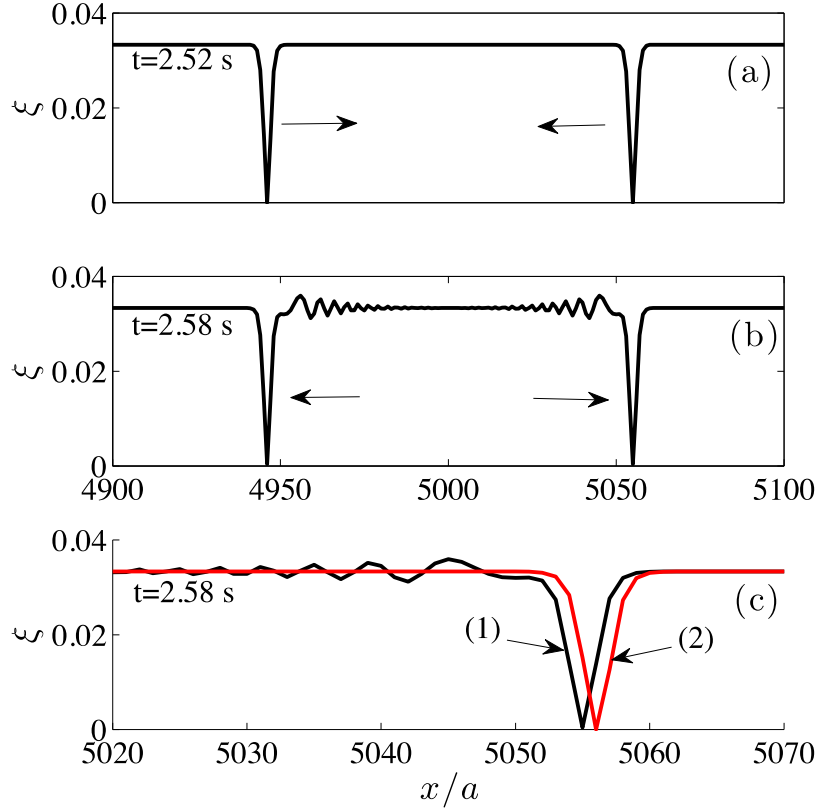
FIG. 2: Development of a two solitary rarefaction strain waves in a chain of 10001 particles compressed with a static force of 4.37 N corresponding to a force-displacement relationship with $n = \frac{1}{2}$, $s = 5 \cdot 10^{-5}$ m, $A = 1 \cdot 10^5$ N/m$^{1/2}$. The initial velocities for the first and last particles are -0.775 and 0.775 m/s. (a) The leading rarefaction pulse separates from the following oscillatory wave train (not shown) after travelling approximately 80 particles. (b) Two rarefaction pulses have crossed leaving an oscillatory tail behind. (c) Results from (b) are compared (curve (1)) with a right moving wave in a chain where there is no collision with a left-moving wave (curve (2)). The minimum strain value of curve (1) is 4e-4 and the phase shift in time between curves (1) and (2) is 0.5 ms.
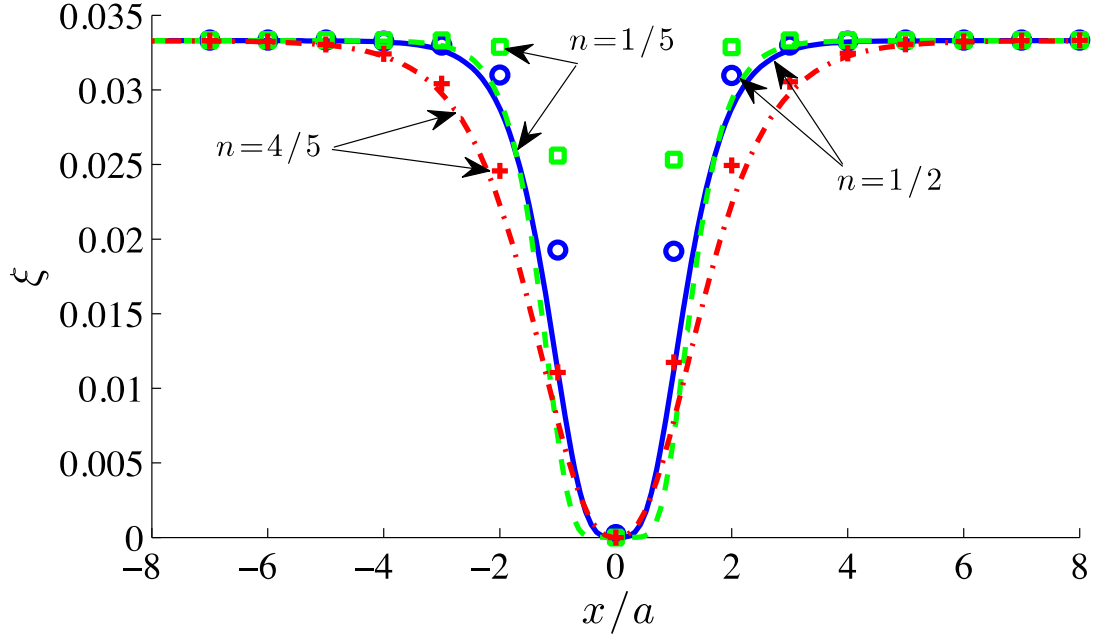
FIG. 3: (color online) Strain from discrete simulations with 1000 particles for $n = 1/5$ (blue O), 1/2 (green □), and 4/5 (red +) is compared to Eq. (9) (corresponding solid lines). The relevant material parameters were $s = 0$ and $A = 1 \cdot 10^5$. Eq. (9) slightly overestimates the width (FWHM) of the solitary rarefaction wave.
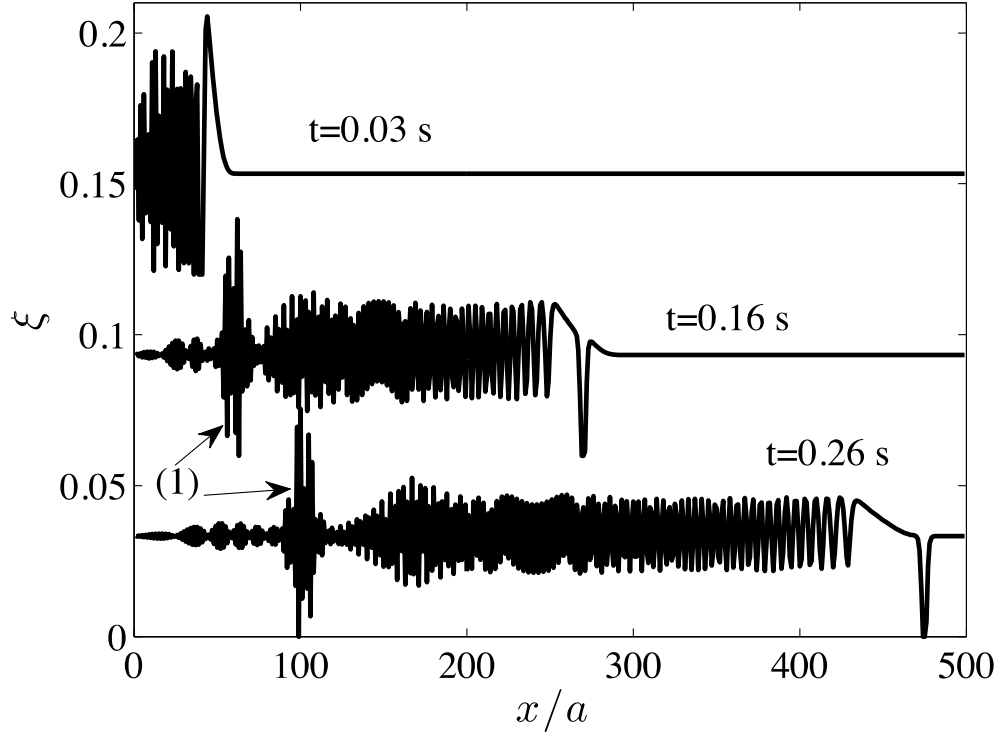
FIG. 4: Impact of a discrete chain of 500 particles at 3 m/s. The chain was compressed with a static force of 4.37 N with $n = 1/2$, $s = 5 \cdot 10^{-5}$ m, $A = 1 \cdot 10^5$ N/m$^{1/2}$. At time t=0.03 s a compression pulse is followed closely by an oscillatory wave train (strain offset by 0.12). At time t=0.16 s a rarefaction pulse is shown passing the compression pulse (strain offset by 0.06). At time t=0.26 s the initial disturbance quickly disintegrates due to nonlinear dispersion into wave packets, periodic waves and the leading rarefaction solitary wave after travelling approximately 475 particles. The strain is offset by 0.12 for visual clarity. The arrow (1) is pointing to a slowly moving wave packet (i.e. an envelope solitary wave).